HIERARCHY OF THERMAL CONDUCTIVITIES FOR ALKALI SILICATES IN TERMS OF IONICITY OF OXYGEN

M. Hayashi, H. Ishii, M. Susa, H. Fukuyama and K. Nagata
TIT, Tokyo, Japan

Abstract

The thermal conductivities of M_2O-SiO_2 (M=Li, Na and K) systems have been measured over a wide temperature range between room temperature and 1573K using the non-stationary hot wire method to investigate the thermal conductivities of alkali silicates in terms of the ionicity of non-bridging oxygen ions. The thermal conductivities at the melting point for the samples having the nominal compositions of 33(mol%)Li_2O-67SiO_2, 33Na_2O-67SiO_2 and 33K_2O-67SiO_2 were recorded as 1.05, 0.73 and 0.55W/mK, respectively. It has been found that silicates containing more ionic non-bridging oxygen ions have smaller thermal conductivites.

Introduction

The mathematical modelling of heat flow in high temperature process is a useful tool to improve process control and product quality. The analysis of the rate of heat flow in refining in iron- and steelmaking industry requires accurate thermophysical data of slags in the solid and liquid states(1,2), among which thermal conductivity is one of the most important data. Thermal conductivity of slags is also of scientific interest because this property is relevant to the silicate network structure.

The relation between the thermal conductivity of silicates and the structure is well explained using Debye's equation. Debye(3) proposed that the thermal conductivity of insulators is expressed as $\lambda=c_v vl/3$ by analogy with kinetic theory of gases, where c_v is the heat capacity at constant volume in J/Km^3, v the speed of sound and l the phonon mean free path. The value of l for silicates is considered to be affected by the number of broken bridges in silica network due to basic oxides. In terms of this, Mills(4) has found a relationship that the thermal conductivity of silicates at the melting point decreases proportionally with an increase in the ratio of the number of non-bridging oxygens per tetrahedrally coordinated atom using previous data. It indicates that the number of broken bridges in silica network is one of the dominant factors controlling the thermal conductivity of silicates.

On the other hand, it has been also reported that silicate glass containing alkali and alkaline earth oxide of lower mass in chemical formula has higher thermal conductivity(5-7). It indicates that the atomic mass of cations of basic oxides is another factor affecting the thermal conductivity of silicates. The atomic mass of cations of basic oxides is relevant to the ionicity of non-bridging oxygen ions adjacent to cations (M): As non-bridging oxygen ions are more ionic, the bonding energy of M-O bond, i.e., the attraction force between M and O ions, is smaller. As a result, phonons would travel less easily from one network unit to another, leading to smaller thermal conductivity. However, to the best of our knowledge, there is no previous investigation about the effect of the ionicity of non-bridging oxygen ions on the thermal conductivity of silicates.

The thermal conductivity of silicate glass might not be determined uniquely because the glass is in a non-equilibrium state. On the other hand, silicate melt at the melting point is in equilibrium and has a structure close to the structure of the glass, which has been studied more widely and profoundly than that of the melt. Therefore, thermal conductivities of various silicates should be compared and discussed using the values at the melting point based upon the conventional theory of glass structure. The aim of this study is to measure thermal conductivities at the melting point for the M_2O-SiO_2 (M = Li, Na and K) systems having the same non-bridging oxygen ion content to investigate the effect of the ionicity of non-bridging oxygen ions on the thermal conductivites of molten alkali silicates. In this work, the ionic refractivity of oxygen (R_O)(8) is used as a measure of the ionicity of non-bridging oxygen ions. The value of R_O, calculated using densities and refractive indices of silicates, is proportional to the average electronic polarisability of bridging and non-bridging oxygen ions. If the fraction of non-bridging oxygen ions to the total oxygen ions is constant, larger values of R_O indicate that non-bridging oxygen ions have larger electron densities and are more ionic.

Experimental

Sample preparation

Master glasses of 33(mol%)M_2O-67SiO_2 (M = Li, Na and K) were prepared from reagent grade SiO_2, Li_2CO_3, Na_2CO_3 and K_2CO_3 powders. Powders were dried enough at elevated

temperatures. Weighed mixtures of SiO_2 and carbonates were placed in platinum crucibles and melted in air for 1h at temperatures between 1573 and 1773K, depending on the composition. After being degassed, glassy samples were prepared by pouring the melts onto a water-cooled copper plate and then crushed up. Subsequently, the glasses were melted again for 1h at the above temperatures to ensure homogenization and quenched again in the same manner as the above way to obtain the samples.

Measurement

The thermal conductivity of the silicates was measured using the non-stationary hot wire method, as shown in Figure 1. In this method, electrical power is supplied to a thin metal wire (hot wire) placed in the sample, which serves as both a heating element and a temperature sensor, and the temperature rise (ΔT) of the wire is recorded continuously. The thermal conductivity of the sample (λ) is obtained from Eq.(1)(9)

$$\Delta T = \frac{Q}{4\pi\lambda}\left(\ln t + A\right) \tag{1}$$

where Q is the heat generation rate per unit length of the wire, t the time and A a constant. In practice, the thermal conductivity of the sample is derived using the slope of the linear portion of the relation betweenΔT and ln$t$ from Eq.(2).

$$\lambda = \frac{Q}{4\pi}\Big/\frac{d\Delta T}{d\ln t} \tag{2}$$

As shown in Figure 1, the sample was held in a cylindrical alumina crucible (24mm in inner diameter) in the furnace. To suppress steady convection during the measurement of molten silicates, the surface temperature of the samples was kept higher by about 10K than the bottom temperature. The probe was immersed vertically into the sample so that the hot wire was placed in the centre of the sample. The probe consisted of a hot wire (0.15mm in diameter and 40-50mm in length) of platinum-13pct rhodium and two platinum potential leads (0.15mm in diameter) attached at an interval of 15-25mm to the hot wire, to allow four-terminal resistance measurements. These wires were connected to platinum rods of 2.0mm in diameter and platinum lead wires of 0.5mm in diameter.

The current of 0.9-1.3A and 1.3-2.0A was supplied to the hot wire via a galvanostat for liquid and solid samples, respectively. The voltage change between the potential wires was monitored continuously using a chart recorder, and was converted to the resistance change of the hot wire based upon the principle of four terminal resistance measurements. The temperature rise (ΔT) was calculated from the resistance change of the hot wire. On the other hand, the heat generation rate per unit length of the hot wire (Q) was calculated from the current and the resistance per unit length of the hot wire at each temperature. Consequently, the thermal conductivity of the sample was derived from Eq.(2), using values of Q and the slope of the linear relationship betweenΔT and ln$t$.

Measurements were carried out over a temperature range between room temperature and 1573K. Measurements were started in air at temperatures 1523, 1573 and 1423K for the Li_2O-SiO_2, Na_2O-SiO_2 and K_2O-SiO_2 systems, respectively, and were carried out during the cooling cycle until the temperatures just below the respective melting points and then during the heating cycle up to the starting temperatures. Subsequently, measurements were made again during the cooling cycle until room temperature and then during the heating cycle up to the temperatures just below the melting points. At least two different probes were used for each sample and two runs were carried out for each system to confirm the reproducibility.

After the measurements, the samples were cooled down in the furnace. It was shown by X-ray diffraction that all the samples were crystallized. Moreover, chemical compositions of the samples were analysed by ICP-AES (Inductively Coupled Plasma-Atomic Emission Spectrometry).

Results

Table 1 shows the chemical compositions of the samples. It is found that during the measurements there was a pickup of alumina in Li_2O-SiO_2 and Na_2O-SiO_2 samples because alumina crucibles were used for the measurements.

Figures 2 and 3 show typical voltage changes (ΔV) versus ln$t$ (a) and the derivative ofΔV with respect to ln$t$, i.e. d(ΔV)/d(ln$t$) versus ln$t$ (b) for solid and liquid Na_2O-SiO_2 samples, respectively. The d(ΔV)/d(ln$t$)-ln$t$ curve is drawn to obtain the slope of the linear portion in the ΔV–ln$t$ curve. In both d(ΔV)/d(ln$t$)-ln$t$ curves plateaus are observed from about 0.6s after the current is supplied. There is a deviation from the plateau in the early stage of measurement. This deviation is associated with the heat capacity of the hot wire itself. In Figure 3(b), there is another deviation from the plateau after 1.4s, which is due to the onset of convection in the molten sample. Calculation of Eq.(2) was carried out using a constant value of d(ΔV)/d(ln$t$) obtained from the plateau of d(ΔV)/d(ln$t$)-ln$t$ curve.

Figure 4 shows the temperature dependence of thermal conductivities of the Na_2O-SiO_2 system. Two different runs are represented by cells 1 and 2. Closed circles and triangles are data recorded during the cooling cycles and open circles and triangles during the heating cycles. The melting point of the sample is indicated by arrow with “m.p.”. The experimental uncertainty is within ±0.1W/mK in the liquid state and ±0.3W/mK or more in the solid state. Previous data(10-12) for Na_2O-SiO_2 systems having the similar compositions are included in Figure 4. Both Kishimoto et al.(11) and Ohta et al.(12) have used the laser flash method, but employed different analytical procedures to eliminate radiation contribution. Nagata and Goto(10) have used the non-stationary hot wire method. Their results are in agreement with the values in this work within the scatter. In the liquid state, the data during the cooling cycles are in good agreement with those during the heating cycles. However, hysterisis is observed in the solid state, which is due to the difference in the degree of crystallization between samples measured during the cooling cycles and those measured during the heating cycles. The thermal conductivity at the melting point for the Na_2O-SiO_2 system is estimated as 0.73 W/mK by interpolation.

Figures 5 and 6 show the temperature dependence of thermal conductivities of the Li_2O-SiO_2 and K_2O-SiO_2 systems, respectively. To the best of our knowledge, there is no previous data for the Li_2O-SiO_2 system. The thermal conductivity of the Li_2O-SiO_2 system has negative temperature dependence, and the relatively larger discrepancy of data is obtained in the solid region between the two cells. On the other hand, the temperature dependence of the thermal conductivity of the K_2O-SiO_2 system is similar to that of the Na_2O-SiO_2 system, and shows hysterisis in the solid state. It is found that the thermal conductivities of silicates in the solid states cannot be determined uniquely due to the difference in the degree of crystallization. The thermal conductivities at the melting point for the Li_2O-SiO_2 and K_2O-SiO_2 systems are estimated as 1.05 and 0.55 W/mK by interpolation.

Discussion

In order to elucidate the effect of structure on the thermal conductivity of silicates, Mills(4) has made a plot of the thermal resistance at the melting point (ρ_m), i.e. the reciprocal of the

thermal conductivity against several structural parameters, and has found that a relationship does exist between ρ_m and these parameters. In silicates there are two types of chemical bonds, i.e. primary covalent bonds between silicon and oxygen in the network structure, and ionic bonds between cations of basic oxides and non-bridging oxygen ions. Thus, the value of ρ_m can be considered to be composed of thermal resistance due to covalent bonds (ρ_{PVB}) and that due to ionic bonds (ρ_{IB}). If x denotes the ratio of non-bridging oxygen (NBO) atoms / (Si+Al atoms), which is a structural parameter proposed by Mysen(13) and denoted by NBO/T, and N denotes the total number of tetrahedral coordinated atoms, then the numbers of covalent and ionic bonds are expressed as $N(4-x)$ and Nx, respectively. The thermal resistance associated with each tetrahedral coordinated atom is described as follows:

$$\rho_m = N(4-x)\rho_{PVB} + Nx\rho_{IB}$$
$$= N(\rho_{IB}-\rho_{PVB})x + 4N\rho_{PVB} \quad (3)$$

As the bonding energy of covalent bond is greater than that of ionic bond, ρ_{PVB} is smaller than ρ_{IB}(14). As proposed by Mills(4), assuming that the values of ρ_{PVB} and ρ_{IB} are independent of compositions, Eq.(3) predicts that the value of ρ_m increases linearly with increasing x, i.e., the value of NBO/T. Figure 7 shows the value of ρ_m as a function of NBO/T(15), which figure is drawn using the data reported by Kishimoto et al.(11), Nagata et al.(10,16) and Sakuraya et al.(17) as well as the data in this work. It can be found that the magnitute of ρ_m is in the hierarchy Li_2O-SiO_2 < Na_2O-SiO_2 < K_2O-SiO_2 despite the similar values of NBO/T. This indicates that the value of ρ_{IB} also depends upon cations of basic oxides. The difference in the value of ρ_{IB} would be caused by the difference in bonding energies between cations of basic oxides and non-bridging oxygen ions. The bonding energy is dependent on the ionic character of chemical bonds between cations and non-bridging oxygen ions, i.e., the ionicity of non-bridging oxygen ions.

The ionic refractivity of oxygen (R_O) is used as a measure of the ionicity of non-bridging oxygen ions. The ionic refractivity of oxygen is calculated by subtracting the ionic refractivities of the respective cations from the molar refractivity of silicates, assuming that the ionic refractivities of cations are constant irrespective of the composition of silicates. The molar refractivity of silicates R can be calculated using Lorentz-Lorenz equation:

$$[(n^2-1)/(n^2+2)]M/\rho = R \quad (4)$$

where n, M and ρ are the refractive index, the molar mass and the density of silicates, respectively. Figure 8 shows the value of ρ_m as a function of R_O, which figure is drawn using the same data as those included in Figure 7. Values of R_O have been calculated using published data for densities and refractive indices measured at room temperature(18) and the ionic refractivities of cations(19). The thermal conductivities of molten silicates should be evaluated using the values of R_O obtained for molten silicates. However, there is no data for densities and refractive indices of molten silicates available for calculating values of R_O. As shown in Figure 8, the thermal resistance increases proportionally with increasing the value of R_O, indicating that silicates containing more ionic non-bridging oxygen ions have smaller thermal conductivities. Consequently, it can be concluded that the ionicity of non-bridging oxygen ions is also a factor controlling the thermal conductivity of silicates.

The reported thermal conductivities for the Fe_2O_3-FeO-Al_2O_3-CaO-SiO_2 and fluorosilicate systems are also considered in the same manner as the above way. As fluorosilicates are composed of both oxygen and fluorine ions as anions, the thermal conductivity would be affected not only by the ionicity of non-bridging oxygen ions but also by the ionicity of fluorine ions. Therefore, both the ionic refractivity of oxygen (R_O) and the ionic refractivity of fluorine (R_F) should be used as a measure of the ionicity of anion to interpret the thermal conductivity values. Consider a fluorosilicate glass of xAO-$y$$BF_2$-$z$$SiO_2$, for example, where A

and B represent alkaline earth atoms, and x, y and z are the mole fractions of AO, BF_2 and SiO_2, respectively ($x + y + z = 1$). The molar refractivity of the fluorosilicate R can be expressed as follows:

$$R = xR_{A2+} + yR_{B2+} + zR_{Si4+} + (x + 2z)R_O + 2yR_F \quad (5)$$

Accordingly, the ionic refractivity of anion can be defined as follows:

$$tR_O + (1 - t)R_F = (R - xR_{A2+} - yR_{B2+} - zR_{Si4+}) / (x + 2y + 2z) \quad (6)$$

where $t = (x + 2z) / (x + 2y + 2z)$. This definition is compatible with the definition of R_O for silicates. Figure 9 shows the value of ρ_m as a function of $tR_O + (1 - t)R_F$ using the previous data of the Fe_2O_3-FeO-Al_2O_3-CaO-SiO_2 and fluorosilicate systems(16) as well as the data included in Figures 7 and 8. Values of $tR_O + (1 - t)R_F$ for the Fe_2O_3-FeO-Al_2O_3-CaO-SiO_2 and fluorosilicate systems have been calculated using estimated values of densities and refractive indices and the ionic refractivities of cations(19). Densities were estimated on the basis of additivity using reported values of density for CaO, SiO_2, Al_2O_3, Fe_2O_3, FeO and CaF_2(20). Refractive indices n can be estimated using the following simple empirical relationship(21)

$$\frac{(n-1)}{d} = \sum K_i \frac{W_i}{100} \quad (7)$$

where d is the density (in g/cm^3) of the glass, and W_i and K_i are the mass% and specific refractive index of the various oxides in the glass. Values of K_i for CaO, Fe_2O_3, FeO, Al_2O_3 and SiO_2 are reported as 0.225, 0.308, 0.187, 0.214 and 0.207, respectively. The value of K_i for CaF_2 was estimated as 0.180 using Eq.(7) and published data for densities and refractive indices of the CaO-CaF_2-SiO_2 system(22). It can be seen from Figure 9 that the linear relation exists between the thermal resistance and the value of $tR_O + (1 - t)R_F$, which indicates that the ionicity of fluorine as well as the ionicity of non-bridging oxygen affects the thermal conductivity of fluorosilicates. Nevertheless, the ionic refractivity of fluorine should be more elucidated in terms of the structure of fluorosilicates in order to investigate the relation between thermal conductivity and the ionic refractivity of anion.

Conclusions

The thermal conductivities of the M_2O-SiO_2 (M = Li, Na and K) systems have been measured over a wide temperature range between room temperature and 1573K using the non-stationary hot-wire method.

- The thermal conductivities for 33(mol%)Li_2O-67SiO_2, 33Na_2O-67SiO_2 and 33K_2O-67SiO_2 are 1.05, 0.73 and 0.55W/mK at the respective melting points.
- The thermal resistance at the melting point increases proportionally with increasing the value of the ionic refractivity of oxygen(R_O), which indicates that silicates containing more ionic non-bridging oxygen ions have smaller thermal conductivities.
- The linear relation exists between the thermal resistance at the melting point and the value of $tR_O + (1 - t)R_F$, which indicates that the ionicity of fluorine as well as the ionicity of non-bridging oxygen affects the thermal conductivity of fluorosilicates.

References

1. M. Susa, K.C. Mills, M.J. Richardson, R. Taylor and D. Stewart, *Ironmaking and Steelmaking*, 1994, **21**, 279.
2. M. Susa, K. Nagata and K.C. Mills, *Ironmaking and Steelmaking*, 1993, **20**, 372.
3. P. Debye, Vorträge über die kinetische Theorie der Materie und Elektrizität, Gottinger Wolfskehlvortrage. B. G. Teubner, Leipzig and Berlin, 1914, 46.
4. K.C. Mills, Proc. 3rd Inter. Conf. on Molten Slags and Fluxes, Glasgow, The Institute of Metals, 1989, 59.
5. M.M. Ammar, S. Gharib, M.M. Halawa, Kh. El-Badry, N.A. Ghoneim and H.A. El-Batal, *J. Non-Cryst. Solids*, 1982, **53**, 165.

6. M.M. Ammar, S.A. Gharib, M.M. Halawa, H.A. El-Batal and Kh. El-Badry, *J. Am. Ceram. Soc.*, 1983, **66**, C-76.
7. E.H. Ratcliffe, *Glass Technol.*, 1963, **4**, 113.
8. N. Iwamoto, Y. Makino and S. Kasahara, *J. Non-Cryst. Solids*, 1984, **68**, 379.
9. H.S. Carslaw and J.C. Jaeger, Conduction of Heat in Solids, 2nd. ed., Oxford Univ. Press, 1959, 264.
10. K. Nagata and K.S. Goto, Proc. 2nd Inter. Symp. on Metallurgical Slags and Fluxes, Lake Tahoe, Nevada, The Metallurgical Society of AIME, 1984, 875.
11. M. Kishimoto, M. Maeda, K. Mori and Y. Kawai, Proc. 2nd Inter. Symp. on Metallurgical Slags and Fluxes, Lake Tahoe, Nevada, The Metallurgical Society of AIME, 1984, 891.
12. H. Ohta, Y. Waseda and Y. Shiraishi, Proc. 2nd Inter. Symp. on Metallurgical Slags and Fluxes, Lake Tahoe, Nevada, The Metallurgical Society of AIME, 1984, 863.
13. B.O. Mysen, D. Virgo and C.M. Scarfe, *Am. Mineralogist*, 1980, **65**, 690.
14. K. Eiermann, *Rubber Chem. Technol.*, 1966, **39**, 841.
15. Verein Deutscher Eisenhüttenleute, Slag Atlas, 2nd. ed., Verlag Stahleisen GmbH, 1995, 6.
16. K. Nagata, M. Susa and K.S. Goto, *Tetsu-To-Hagane*, 1983, **69**, 1417.
17. T. Sakuraya, T. Emi, H. Ohta and Y. Waseda, *Nippon-Kinzoku-Gakkaishi*, 1982, **46**, 1131.
18. O.V. Mazurin, M.V. Streltsina and T.P. Shvaiko-Shvaikovskaya, Handbook of Glass Data, Elsevier, 1987.
19. Fanderlik, I. Optical Properties of Glass, Elsevier, 1983, 96.
20. A.N. Winchell and H. Winchell, The Microscopical Characters of Artifical Inorganic Solid Substances, Academic Press, New York, NY, 1964.
21. E.S. Larsen and H. Berman, The Microscopical Determination of Non-opaque Minerals, 2nd edn, US Geological Survey Bull., Washington DC, US Government Printing Office, 1934, 31.
22. N. Iwamoto and Y. Makino, J. Non-Crystall. Solids, 1981, **46**, 81.

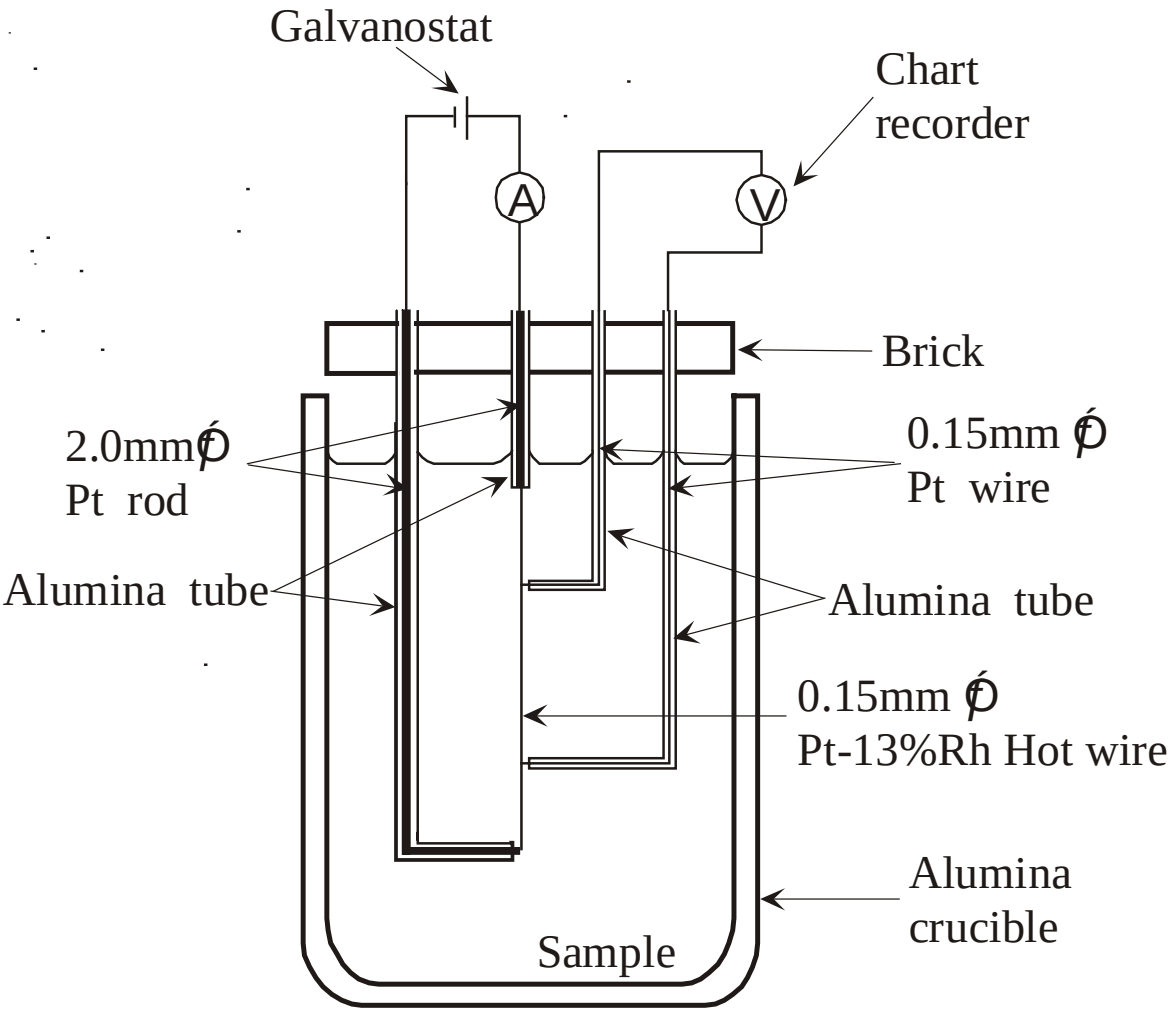

Fig.1 Schematic diagram of the experimental apparatus.

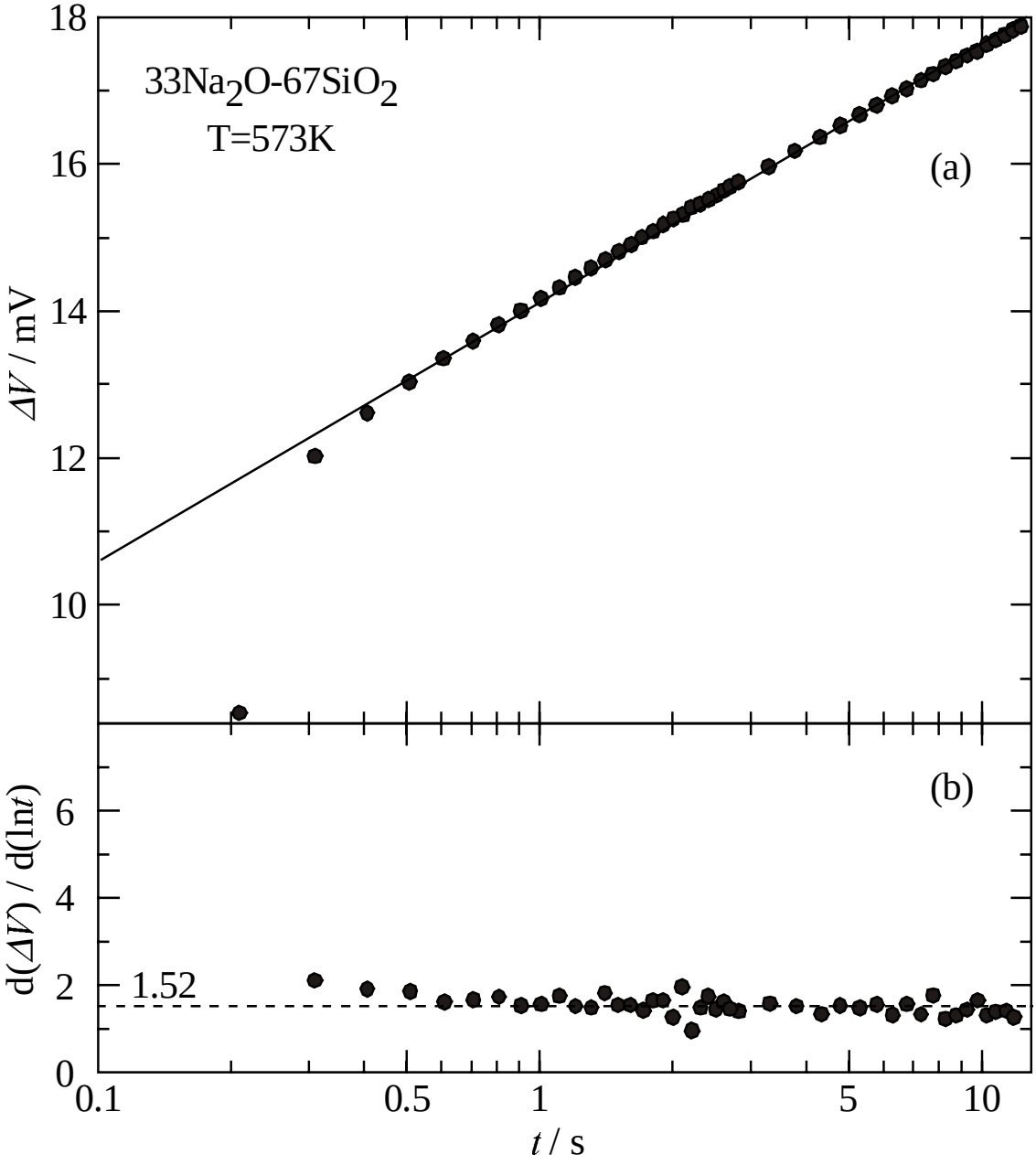

Fig.2 Voltage change (ΔV) versus ln$t$ (a) and d(ΔV)/d(ln$t$) (b) for the Na_2O-SiO_2 system at 573K.

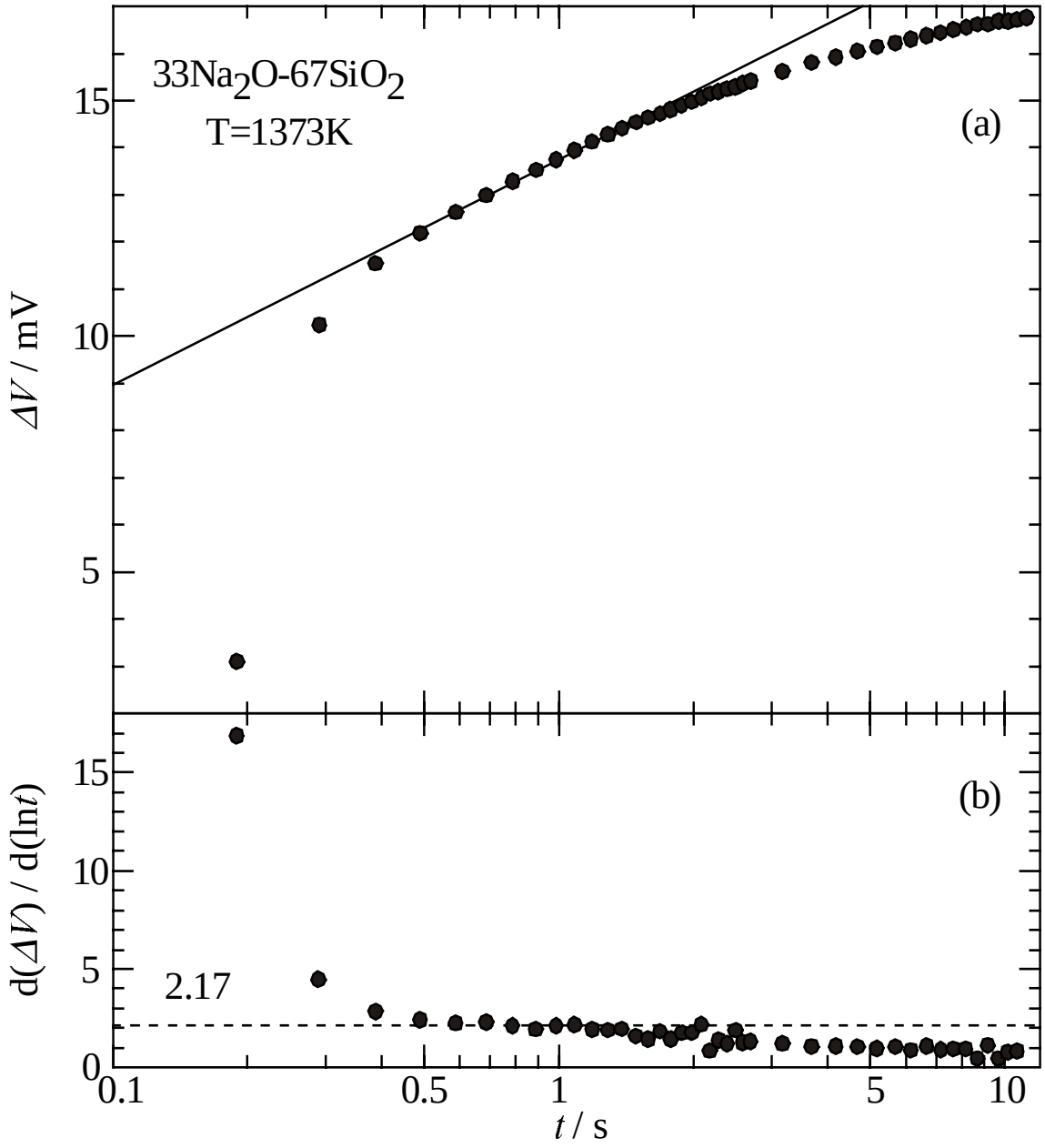

Fig.3 Voltage change (ΔV) versus ln$t$ (a) and d(ΔV)/d(ln$t$) (b) for the Na_2O-SiO_2 system at 1373K.

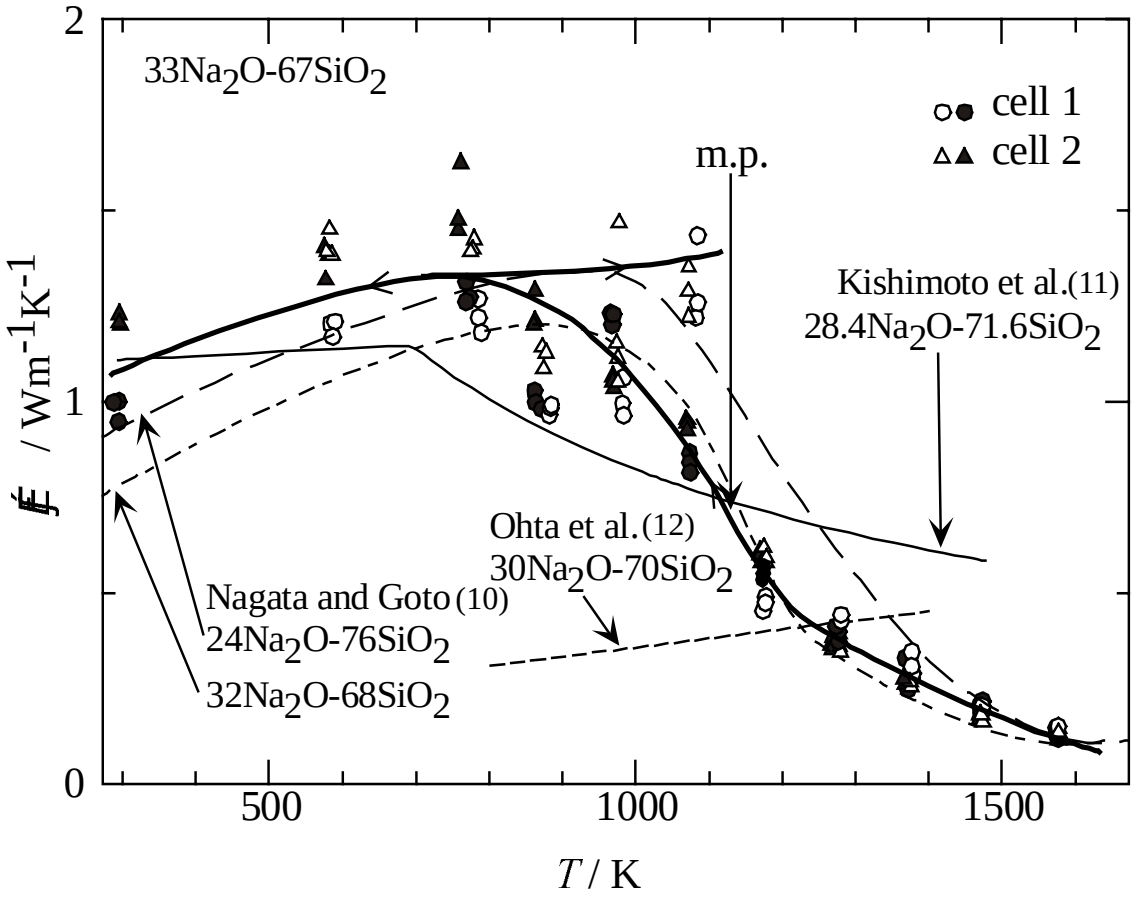

Fig.4 Temperature dependence of the thermal conductivity for the Na_2O-SiO_2 system. Closed circles and triangles are data recorded during the cooling cycles and open circles and triangles during the heating cycles.

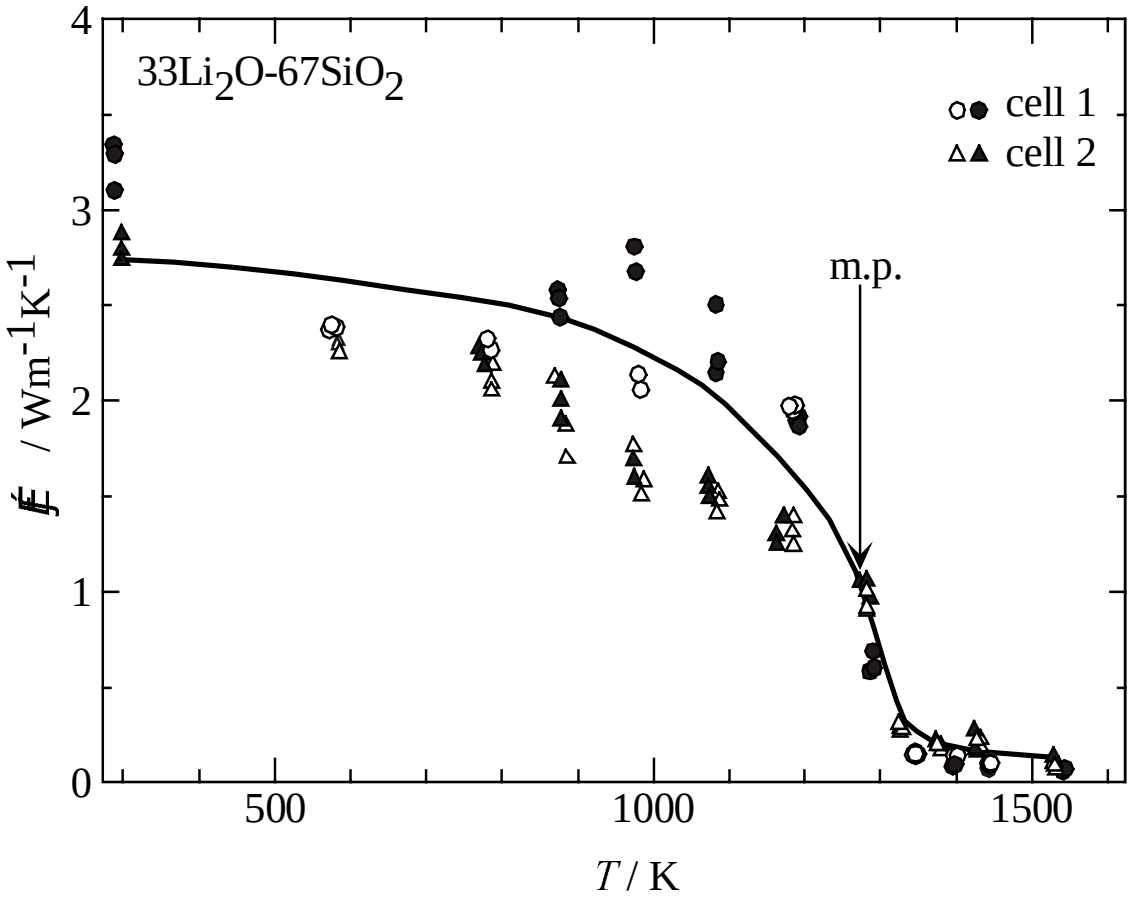

Fig.5 Temperature dependence of the thermal conductivity for the Li_2O-SiO_2 system. Closed circles and triangles are data recorded during the cooling cycles and open circles and triangles during the heating cycles.

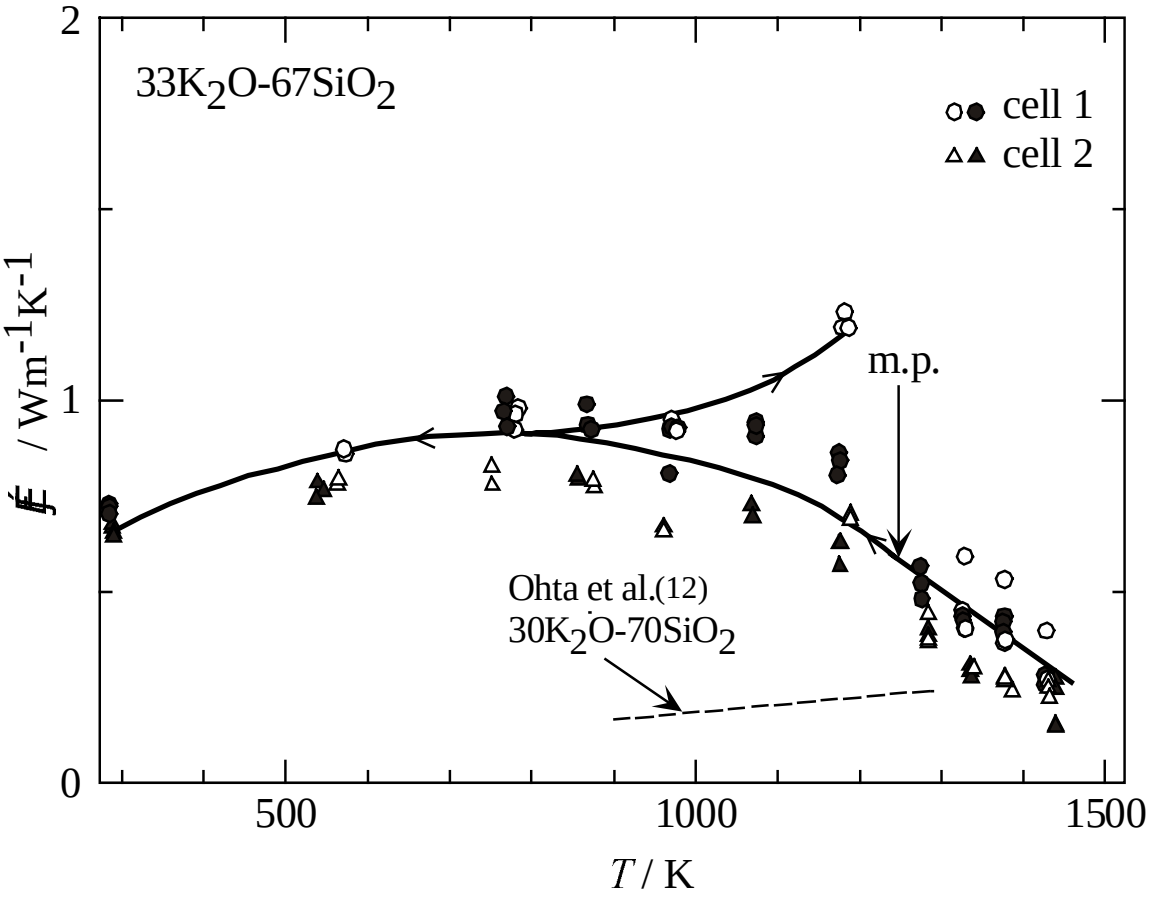

Fig.6 Temperature dependence of the thermal conductivity for the K_2O-SiO_2 system. Closed circles and triangles are data recorded during the cooling cycles and open circles and triangles during the heating cycles.

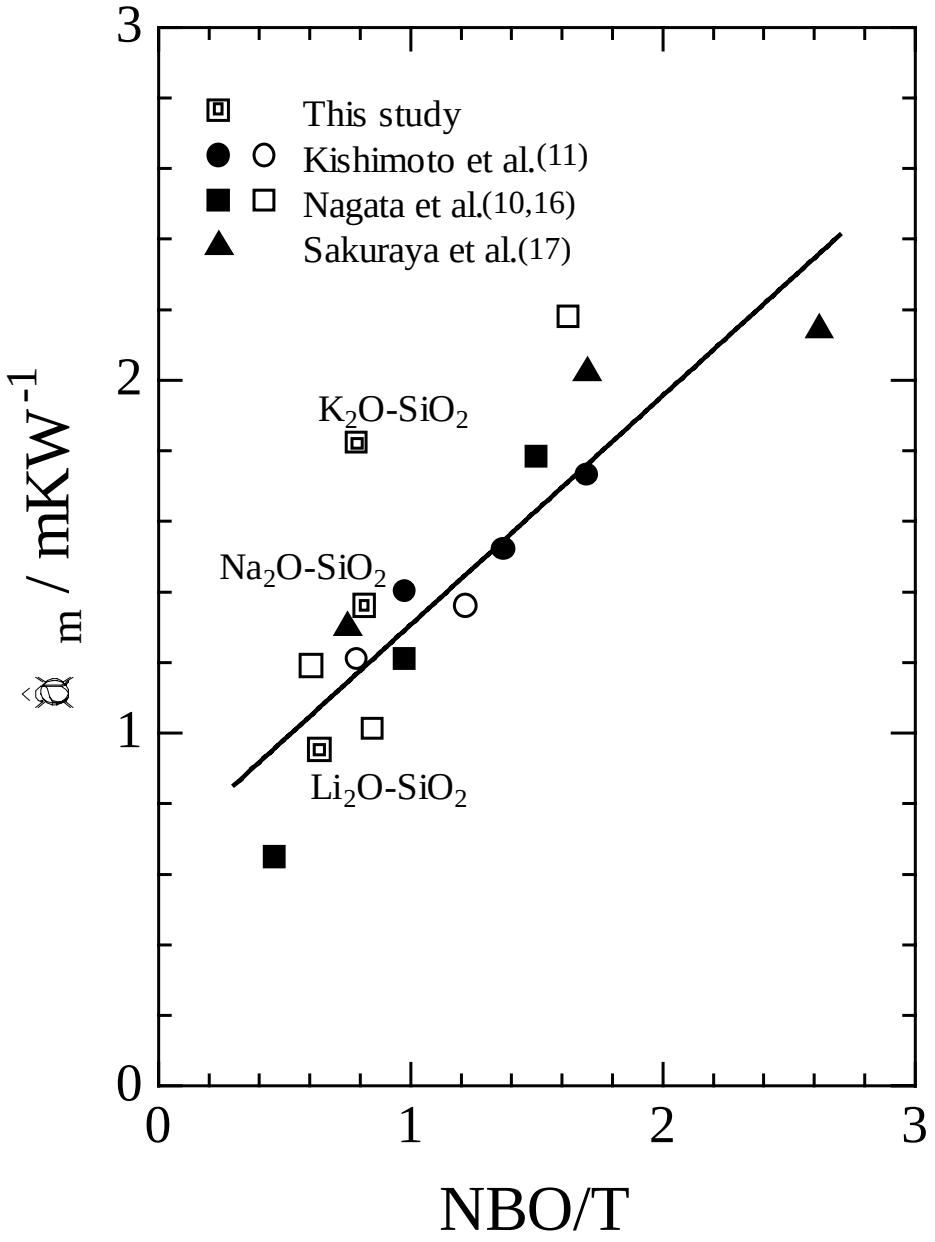

Fig.7 Relation betweenρ_m and the ratio of non-bridging oxygen (NBO) atoms / (Si+Al atoms). Closed circles, closed squares and closed triangles denote data for the $CaO\text{-}Al_2O_3\text{-}SiO_2$ system and open circles and open squares for the $Na_2O\text{-}SiO_2$ system.

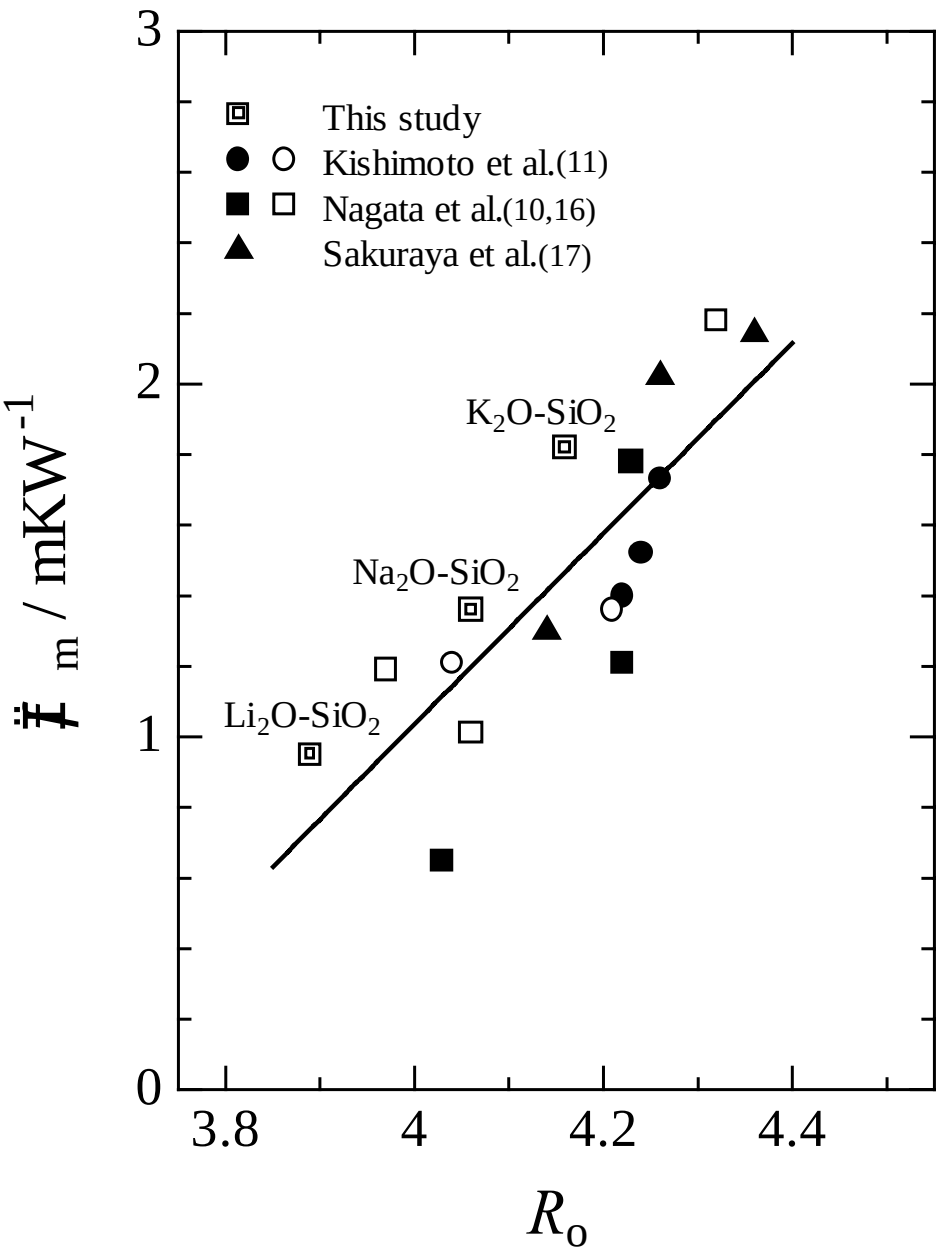

Fig.8 Relation between the values ofρ_m and R_O. Closed circles, closed squares and closed triangles denote data for the $CaO\text{-}Al_2O_3\text{-}SiO_2$ system and open circles and open squares for the $Na_2O\text{-}SiO_2$ system.

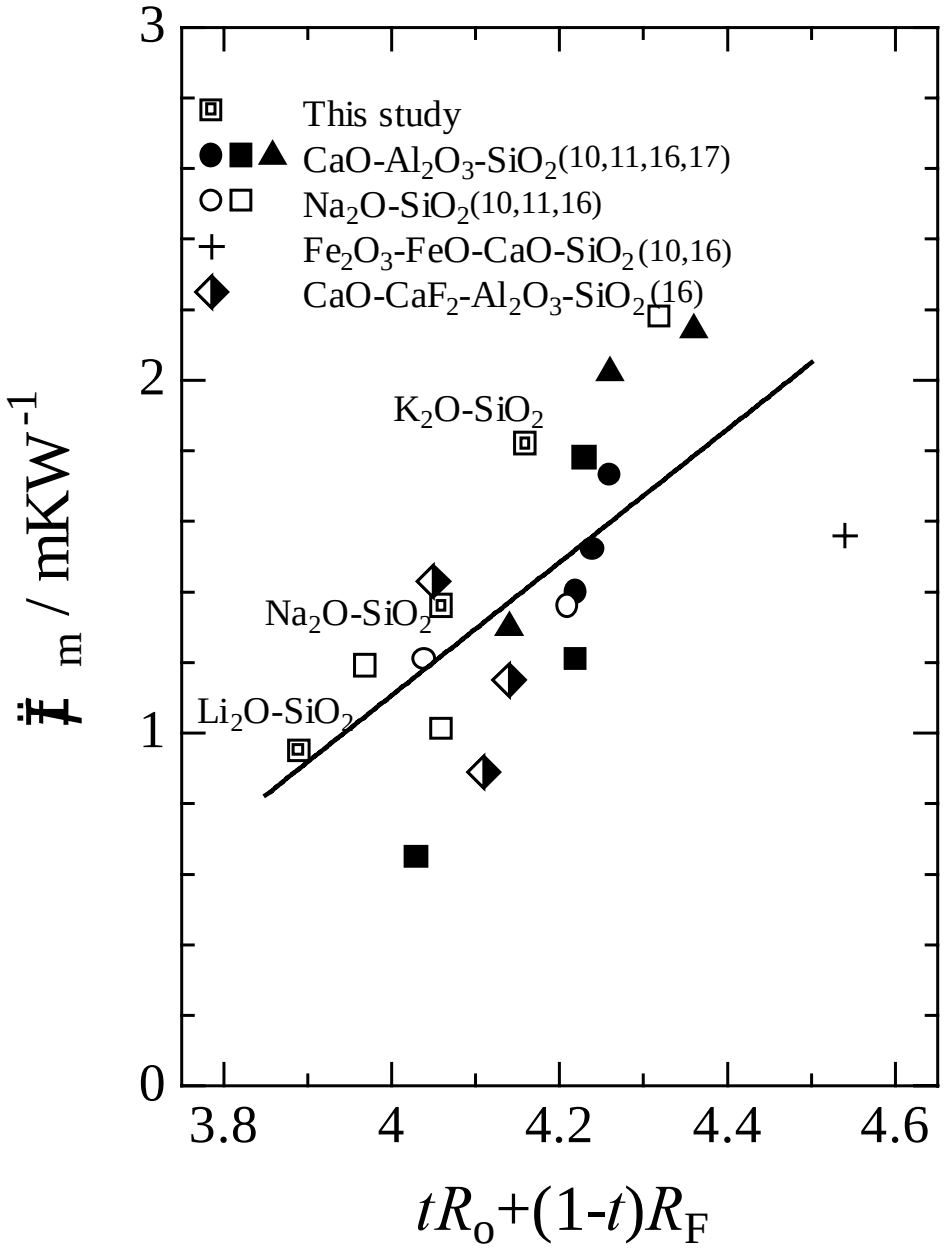

Fig.9 Relation between the values ofρ_m and $tR_O+(1-t)R_F$.

Table 1 Chemical compositions of samples, mol%

Sample	Li_2O	Na_2O	K_2O	SiO_2	Al_2O_3
Li_2O-SiO_2 cell 1	27.6	—	—	67.3	5.1
cell 2	28.4	—	—	69.0	2.6
Na_2O-SiO_2 cell 1	—	29.7	—	69.6	0.7
cell 2	—	28.3	—	70.9	0.8
K_2O-SiO_2 cell 1	—	—	29.0	71.0	—
cell 2	—	—	27.6	72.4	—